Volume 24
Number 18
21 September 2022
Pages 6735-7228

Green Chemistry

Cutting-edge research for a greener sustainable future

rsc.li/greenchem

ISSN 1463-9262

ROYAL SOCIETY OF CHEMISTRY

PAPER

J. Pérez-Ramírez *et al.*

Assessing the environmental benefit of palladium-based single-atom heterogeneous catalysts for Sonogashira coupling

Green Chemistry

PAPER

View Article Online
View Journal | View Issue

Cite this: *Green Chem.*, 2022, **24**, 6879

Assessing the environmental benefit of palladium-based single-atom heterogeneous catalysts for Sonogashira coupling†

D. Faust Akl,‡[a] D. Poier,‡[b] S. C. D'Angelo, [a] T. P. Araújo,[a] V. Tulus, [a] O. V. Safonova, [c] S. Mitchell, *[a] R. Marti,*[b] G. Guillén-Gosálbez *[a] and J. Pérez-Ramírez *[a]

The Pd–Cu catalysed Sonogashira coupling of terminal alkynes and aryl halides is a cornerstone synthetic strategy for C–C bond formation. Homogeneous organometallic systems conventionally applied are typically not reusable and require efficient downstream Pd removal steps for product purification, making it challenging to fully recover the precious metal. A holistic cradle-to-gate life cycle assessment (LCA) unveils that process footprint can be improved up to two orders of magnitude from repeated catalyst reuse. New classes of heterogeneous catalysts based on isolated metal atoms (single-atom catalysts, SACs) demonstrate promising potential to synergise the benefits of solid and molecular catalysts for efficient Pd utilisation. Here we show that using Pd atoms anchored on nitrogen-doped carbon permits full recovery of the metal and reuse of the catalyst over multiple cycles. A hybrid process using the Pd-SAC with a homogeneous CuI cocatalyst is more effective than a fully heterogeneous analogue based on a bimetallic Pd–Cu SAC, which deactivates severely due to copper leaching. In some scenarios, the LCA-based metrics demonstrate the footprint of the hybrid homogeneous–heterogeneous catalytic process is leaner than the purely homogeneous counterpart already upon single reuse. Combining LCA with experimental evaluation will be a useful guide to the implementation of solid, reusable catalysts for sustainable organic transformations.

Received 17th May 2022,
Accepted 29th June 2022

DOI: 10.1039/d2gc01853e

rsc.li/greenchem

Introduction

Many active pharmaceutical ingredients (API), or intermediates thereof, contain alkyne groups readily accessible through the Sonogashira C–C cross-coupling reaction[1] between aryl halides and substituted alkynes.[2–6] Organometallic palladium complexes (commonly $Pd(PPh_3)_4$ or $Pd(OAc)_2$, Ph – phenyl, OAc – acetate) are the prevailing catalysts employed in this class of organic transformation with high productivity and selectivity across a range of substrates. Despite improving chemical manufacturing process sustainability through shortened synthesis routes and the avoidance of stoichiometric reagents,[7] single-use palladium catalysts have operational and environmental ramifications. Strict limitations on permissible palladium traces in pharmaceutical products mandate efficient removal steps, either realised through thermal separation units (*e.g.*, crystallisation)[7] or more elaborated metal scavenging systems (solid or liquid).[8] The additional process steps, which also increase costs (*e.g.*, CAPEX, energy), burden the environmental footprint through increased amounts of waste produced (*e.g.*, solvent, scavenger material)[9] and potentially inhibited palladium recovery.

These issues are being addressed for organometallic catalysts by reducing the employed palladium quantities[10] or enabling the use of aqueous micellar catalysts,[11,12] among others. Alternatively, catalyst reusability, simplified product separation, and effective metal recovery routes[13] motivate the search for solid catalytic materials with equivalent performance. Achieving this goal is challenging due to the typically lower molecular-level uniformity of conventional heterogeneous catalysts, such as palladium nanoparticles (*e.g.*, palladium on charcoal),[14] which often results in an inferior specific activity. Furthermore, metal leaching is a common problem.[15–17] Remarkably, organometallic and heterogeneous catalysts have not been compared in a broader context beyond simple, performance-based heuristics.

[a]*Institute for Chemical and Bioengineering, Department of Chemistry and Applied Biosciences, ETH Zurich, Vladimir-Prelog-Weg 1, 8093 Zurich, Switzerland. E-mail: msharon@chem.ethz.ch, gonzalo.guillen@chem.ethz.ch, jpr@chem.ethz.ch*
[b]*Institute of Chemical Technology, University of Applied Sciences and Arts of Western Switzerland Fribourg, Boulevard de Pérolles 80, 1700 Fribourg, Switzerland. E-mail: roger.marti@hefr.ch*
[c]*Paul-Scherrer Institute, Forschungsstrasse 111, 5232 Villigen PSI, Switzerland*

†Electronic supplementary information (ESI) available: Additional characterisation of the catalysts, reagents and products, and description of standard reaction procedures. See DOI: https://doi.org/10.1039/d2gc01853e

‡These authors contributed equally to this work.

The preferred approach to evaluate the environmental footprint of (fine) chemical processes is to carry out a life cycle assessment (LCA) study. However, the main focus is set on quantifying the impact of reactants, solvents, utilities, direct emissions, and waste, while the contribution of the catalyst, although identified as significant,[18–20] has been often neglected. In particular, the importance of durability of solid catalysts in continuous operation,[18] noble metal loading[21] and recovery[22,23] for key sustainability metrics is not reflected in most catalyst design efforts. Despite the growing need to quantify the environmental metrics of new technologies, studies combining experiments and LCA remain scarce.[24,25]

Significant advances in characterisation and synthesis techniques have vastly expanded the design space for catalytic materials. Among these trends, more well-defined active sites in single-atom heterogeneous catalysts (SAC) and therewith associated high and tailorable selectivity compared to conventional nanoparticle analogues,[26] attracts interest to replace organometallic catalysts in organic transformations.[27,28] However, only a few studies have tackled the design of SACs for the Sonogashira reaction. In work using Heck–Cassar-like conditions (copper-free Sonogashira), a palladium SAC on titania (anatase) achieved quantitative conversion (90% selectivity) when using substituted iodoaryls, thereby improving on a nanoparticle-containing analogue. Attempts to reactivate the catalyst between runs did not prevent the decreasing activity observed at constant selectivity.[29] Remarkably, carbon-based carriers such as nitrogen-doped carbon (NC) or graphitic carbon nitride (GCN), which are the most prominent single-atom catalyst carriers due to their high surface area and density of surface coordination sites,[26,30,31] have not been explored in the Sonogashira reaction.

Here, we quantify the potential benefit of using palladium-based heterogeneous catalysts compared to homogeneous analogues for the Sonogashira coupling reaction based on metrics obtained from a holistic cradle-to-gate life cycle analysis. Prompted by the significantly reduced possible impact, we evaluate atomically dispersed palladium on chemically-distinct carriers, comparing the performance to commonly applied homogeneous systems. Seeking the potential use of a purely solid catalyst, different modes of copper introduction, *i.e.*, as a soluble salt (CuI) or in the form of a bimetallic palladium-copper SAC, are considered. Benchmarking under an optimised Sonogashira reaction protocol highlights the interplay between catalyst activity and stability and the critical role of ensuring proximity between copper and palladium species. Our study highlights the environmental savings that this technology could bring to fine chemicals production and identifies challenges for catalyst design.

Methods

Life cycle assessment

The potential environmental performance of a SAC-based Sonogashira process was quantified through the application of LCA principles following the ISO 14044:2006 standard (see scheme in Fig. S1†).[32] LCA phase one involved a cradle-to-gate assessment, encompassing all upstream activities associated with catalyst synthesis, use, and recovery and omitting further transformation of the products of this reaction into other compounds. The functional unit is 1 ton of product **3**, $ton_{(3)}$; contributions from by-products are not considered. Two processes were compared, the fully homogeneously catalysed batch reaction (CuI, business as usual reference) and the hybrid-SAC (Pd/NC, CuI) catalysed analogue. As a baseline, it was assumed that the heterogeneous catalyst could be re-used for 100 batches, before noble metal recovery and refining, whereas the homogeneous catalyst had to undergo this process after every catalytic run. Three scenarios considered distinct palladium recovery: no recovery (**A**), low recovery (**B**), and high recovery (**C**). All materials (*e.g.*, reactants, cocatalysts, products, and solvent) except for the catalyst were assumed to be used in the same quantity across scenarios. Additional scenarios considered (i) catalyst deactivation and (ii) metal leaching. In the former, the decrease of catalytic activity as a function of the catalytic run was assumed to be constant; the palladium content of the catalyst remains unchanged. Metal leaching was approximated through an exponential decay in palladium content as a function of the catalytic run. The palladium lost in each run is not recovered and cannot contribute to the catalytic activity.

The life cycle inventories (LCIs) for the two processes (LCA phase two) were obtained by combining the mass flows retrieved from the experimental data (foreground system) with data from ecoinvent v3.5 (background system).[33] The impact of the catalyst was approximated with the impact associated with the metal it contained, which is the main factor that varies drastically across the considered scenarios. For the base case scenario, the sole impact of palladium was considered to be relevant. Although CuI could be completely regenerated, it was assumed to be used as a stoichiometric reagent, and its impact, as well as the one from wastewater treatment are reported (Table S1†). Our estimates, therefore, provide a lower bound on the true impact that would result from a more detailed LCA at later stages of process development, when more accurate data become available.

In terms of impact assessment (LCA phase three), we considered impacts on the global warming potential (GWP), quantified as a midpoint of the ReCiPe 2016 methodology,[34] as well as the three endpoints of the same approach, namely human health (HH), ecosystem quality (EQ), and resource scarcity (Res). GWP impacts are quantified in $ton_{CO2\text{-}eq}$ and correspond to the amount of greenhouse gas released into the atmosphere throughout the life cycle steps included in the selected system boundaries; HH damages, expressed in disability-adjusted life years (DALYs), correspond to the time that a person is disabled due to disease or accident; EQ damages are expressed in local species loss integrated over time (species-yr); finally, Res, quantified in USD, denote the extra costs involved in future mineral and fossil resource extraction due to the current exploitation of resources.

Catalyst preparation

Single-atom heterogeneous catalysts were prepared adapting previously reported procedures.[35] Carriers (nitrogen-doped carbon, exfoliated carbon nitride, aluminium oxide, activated carbon) were impregnated with an appropriate amount (0.5 wt% nominal palladium loading) of the palladium precursor using previously reported impregnation methods. The obtained solids were dried overnight (338 K) and annealed in a tubular oven under nitrogen flow (573 K, 5 h hold, 5 K min^{-1} ramp). For the preparation of bimetallic PdCu-SACs, Pd and Cu were impregnated onto the selected carriers sequentially. Full details of the catalyst preparation and characterisation are provided in Note S1.†

Catalyst evaluation

Chemicals. All chemicals were acquired from Chemie Brunschwig AG and Merck and used without further purification.

Sonogashira coupling reaction. Aside from the SACs, the following benchmark systems were included in the catalytic tests: Pd_{NP}/C (10 wt% palladium content, Sigma-Aldrich, Lot MKBV2219 V), $PdCl_2(P(C_6H_5)_3)_2$ (Acros Organics), Pd $(P(C_6H_5)_3)_4$ (Sigma-Aldrich), and $Pd(CH_3COO)_2$ (Acros Organics). Unless otherwise stated, the Sonogashira coupling reaction was performed following a standard procedure: a degassed solution consisting of iodobenzene (1 equivalent, eq.), phenylacetylene (1.1 eq.), base (2.2 eq.), 1,3,5-trimethylbenzene (0.25 eq., internal standard), and solvent (0.5 M) was added to the palladium catalyst (0.1 mol%, 0.5 wt% palladium content for SAC), copper(I) iodide (1 mol%), and ligand (1 mol%), and vigorously stirred for 24 h at 353 K under a protective atmosphere (Ar). After cooling to room temperature, the SAC was separated from the reaction mixture by filtration. The reaction solution was analysed by gas chromatography (GC), performed on a Thermo TRACE 1300 chromatograph equipped with a flame ionisation detector, and a ZB-5 column (5%-phenyl-95%-dimethylpolysiloxane, 30 m length, 0.25 mm inner diameter, 0.25 μm film thickness) using helium as carrier gas. Further details on the product analysis and standard conditions for catalyst evaluation are described in Notes S1–S3.†

Results and discussion

Footprint of Pd-catalysed Sonogashira reaction

A cradle-to-gate life cycle analysis (LCA) was conducted to assess the potential economic and environmental benefits of using heterogeneous *versus* homogeneous (*i.e.*, organometallic complex) palladium catalysts in organic transformations. In the presented case, we considered the copper-cocatalysed Sonogashira coupling of aryl iodides and aryl alkynes with the catalytic systems presented below (reaction scheme in Fig. 1a). However, the framework of the assessment is generally applicable to other coupling reactions. Although a detailed process modelling was not possible due to data gaps, a brief analysis

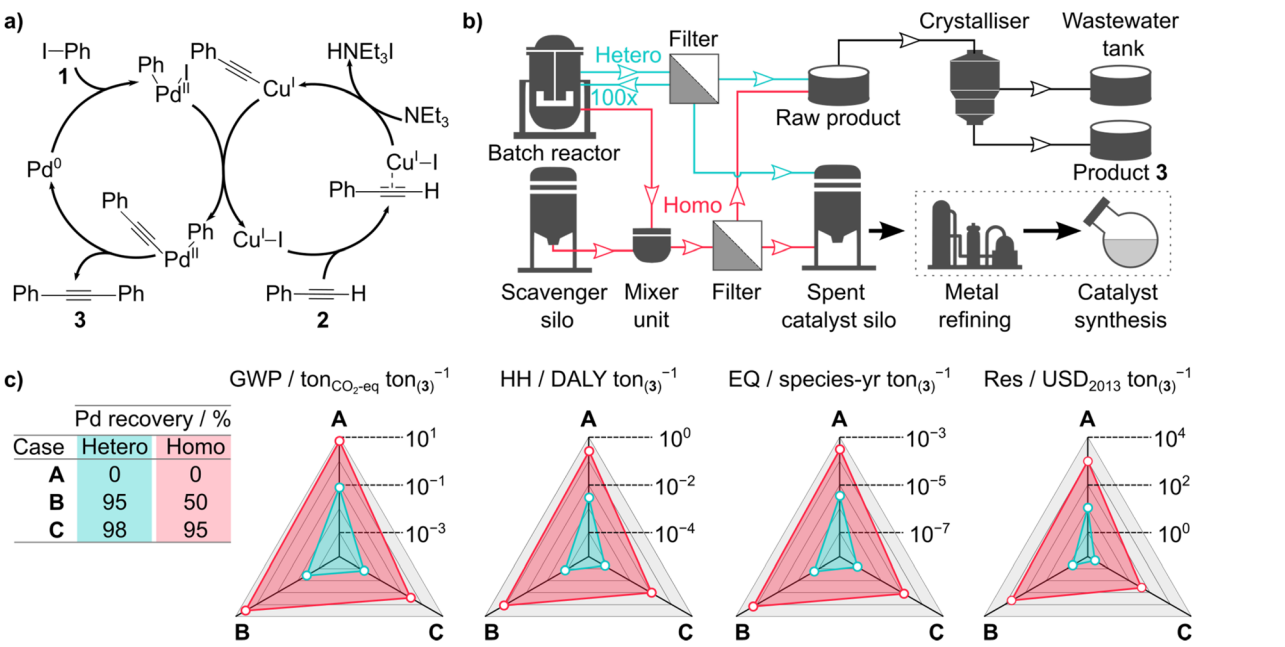

Fig. 1 (a) Schematic of the classical catalytic cycle of the Cu-cocatalysed Sonogashira reaction. (b) Unit operation scheme of a hypothetical Sonogashira process, with key differences depending on the choice of a homogeneous (red) or heterogeneous (turquoise) catalyst highlighted. (c) Comparison of the impact of palladium consumption associated with using a homogeneous or heterogeneous catalyst for Sonogashira coupling. Three different recovery cases are considered based on four sustainability metrics: the Midpoint Global Warming Potential (GWP) and the Endpoints Human Health (HH), Ecosystems Quality (EQ), and Resources (Res). The base case considers 100 recycles for the heterogeneous catalyst and direct disposal of the homogeneous catalyst after each run. Reported values are per ton of product 3 ($kg_{(3)}$). The colour code in (b) applies to (c).

revealed the employed copper cocatalyst and waste-water treatment have negligible impact compared to the environmental burden associated with the use of palladium (*e.g.*, GWP of 7370 $ton_{CO2\text{-}eq}$ ton_{Pd}^{-1}, Table S1†).

Hence, analysing the central aspect of palladium (re)utilisation when using heterogeneous or homogeneous catalysts can help determine the potential environmental benefits. When visualised on a (hypothetical) process level (Fig. 1b), the heterogeneous catalyst could be separated from the reaction mixture (*e.g.*, filtering) and reconditioned for reuse (*e.g.*, through washing or heating). After the end of its useable life (100 catalytic runs), the catalyst would be transferred to a metal refining facility, where palladium could be recovered, usually in the form of a highly acidic solution, purified and processed into precursors suited for catalyst synthesis. Unfortunately, quantitative analyses of process steps involved in palladium recovery are scarce in the open literature. Nonetheless, precious metal recovery from solid catalysts is known to be highly optimised and efficient.[34,36] In the case of the organometallic catalyst, product purification might occur through solid palladium scavengers or more elaborate thermal separation operations (*e.g.*, crystallisation, distillation). As for the heterogeneous catalyst, the palladium-containing scavenger or liquid waste streams would be subsequently refined, followed by catalyst synthesis. Although not considered in detail, we expect downstream palladium recovery and refining (*e.g.*, energy requirement and waste streams) to be similar for both process alternatives when using an efficient solid palladium scavenger. In certain circumstances, metal recovery may be economically unfeasible. In particular, from liquid streams containing low concentrations of organometallic catalyst (*e.g.*, reduced catalyst input), when the product stream is highly diluted or due to solubility differences in biphasic systems. Discarding dilute streams will lead to low recovery rates (50%), requiring external palladium inputs for synthesising a new batch of catalyst.

Hence, the main distinctions between the heterogeneously and homogeneously catalysed processes are the number of catalyst reuses (100 or 0, respectively), and the different palladium recovery capacities. Specifically, we considered three scenarios for metal recovery after the useful catalyst life: **A** no palladium recovery (*i.e.*, full replacement of the palladium input), **B** unfavourable palladium recovery (*e.g.*, when only part of the waste stream is processed), and **C** good palladium recovery. As the production of pure palladium is resource intensive, its impact on the midpoint global warming potential (GWP), and endpoint categories of human health (HH), ecosystems quality (EQ), and resources (Res) decreases with increasing metal recovery rate independently of the considered catalyst (Fig. 1c). For all metrics, the footprint of a heterogeneously-catalysed process would be at least two orders of magnitude lower than a homogeneously catalysed analogue. In particular, the impact of the heterogeneous case was found to be about 0.11, 1.1, or 5.6% of that of the homogeneous for scenarios **B**, **A**, and **C**, respectively. The biggest spread between both catalytic systems arose for the worst case palladium recovery scenario (**B**) and correlated closely with the imposed recovery rates. Specifically, the performance for scenario **C** equals about 8% (homogeneous) and 40% (heterogeneous) of the respective performance for scenario **B**. Under a more conservative scenario with no CuI recovery and adding the impact of copper onto the GWP as a representative metric (see Table S1† for other metrics), the homogeneous process footprint becomes 6, 56, or even 68 times the one of the heterogeneous counterpart for scenarios **C**, **A**, and **B**, respectively.

Since the development of heterogeneous catalysts for organic transformations such as the Sonogashira reaction is still in its infancy, the stability may not be sufficient to permit reuse in 100 cycles. To provide a broader guideline for productivity, we analysed the GWP sensitivity towards catalyst recyclability (Fig. 2). In the most unfavourable case (scenario **A**, without palladium recovery) a solid catalyst stable over 30 catalytic runs outperformed the GWP of the organometallic benchmark. Comparatively, assuming typical metal recovery efficiency (scenario **B**), the possibility to reuse the catalyst in two catalytic runs was already sufficient to improve sustainability. For a scenario, where a more active organometallic catalyst reduces the required palladium input, the minimum number of catalytic recycles of a competing heterogeneous catalyst would need to increase accordingly. The environmental benefit obtained from reusing the heterogeneous catalyst diminished when considering catalyst activity loss or palladium leaching. Specifically, catalyst deactivation without metal loss limited the useful catalyst lifetime and reduced the yield per catalytic run (Fig. 2b). The effect on the process GWP scaled with the deactivation rate. Nonetheless, catalyst reuse still reduced overall impact. Both activity and metal recovery are affected in a scenario with partial loss of palladium through leaching in every catalytic run (Fig. 2c). Compared to the scenario with constant deactivation, the overall GWP level increased and surpassed the values of the homogeneous catalyst from leaching rates of 5%. Repeated catalyst reuse only resulted in a marginally improved environmental footprint in terms of GWP. Clearly, the loss of palladium into solution, which is assumed to not be recoverable, offsets the benefits of a heterogeneous catalyst over a homogeneous benchmark. Hence, the LCA disclosed non-trivial heterogeneous catalyst selection criteria, namely the necessity to ensure high palladium recovery rates, while tolerating deactivation in the absence of metal leaching. The use of a heterogeneous catalyst is particularly attractive if the precious metal is difficult to recover in the homogeneously-catalysed analogous process.

Preparation of single-atom heterogeneous catalysts (SACs)

As a promising class of catalytic materials for organic transformations,[26] we evaluated palladium SACs prepared through a standard wet impregnation method using common, chemically-distinct carrier materials (Tables S2 and S3,† Fig. 3 and Fig. S2–S4†), namely activated carbon (AC), exfoliated graphitic carbon nitride (ECN), aluminium oxide (Al_2O_3), and nitrogen-doped carbon (NC). Because SACs based on NC were found to yield the best performance (see below), the co-introduction of

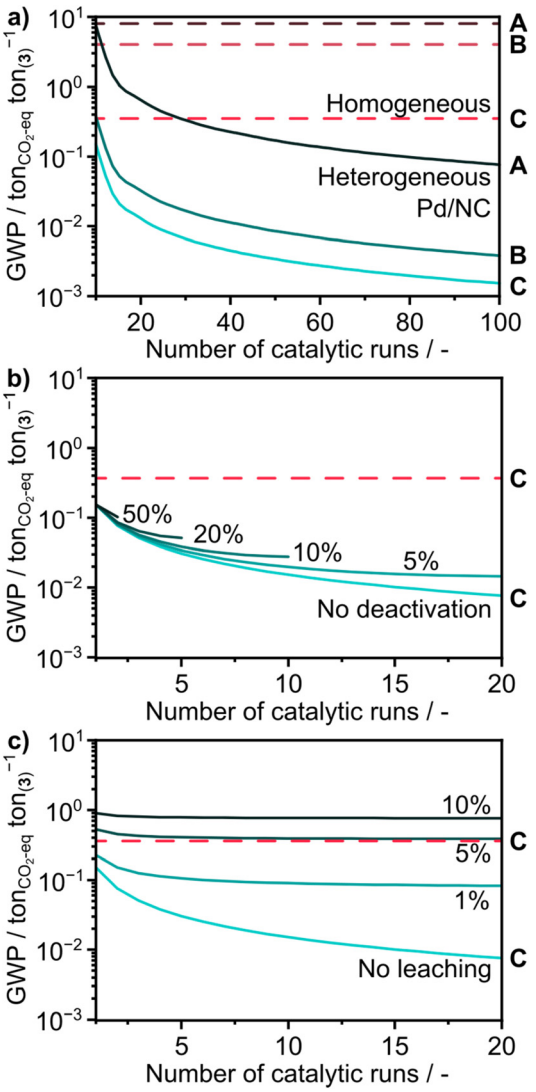

Fig. 2 (a) Sensitivity analysis of the number of catalytic runs feasible with a heterogeneous catalyst on the Global Warming Potential (GWP) of the process assuming palladium recovery rates specified in Fig. 1. (b) Impact of constant heterogeneous catalyst deactivation on the GWP trajectory of scenario C as a function of the number of catalytic runs. Palladium leaching was assumed to be absent. (c) Sensitivity of GWP on the number of catalytic runs of a heterogeneous catalyst suffering from different degrees of palladium loss during reaction. Leaching was considered to affect catalyst activity and recoverable palladium quantities.

copper to obtain a fully heterogeneous, bimetallic catalyst was pursued. The resulting Cu : Pd molar ratio in PdCu/NC closely matched the standard ratios employed in Sonogashira reaction protocols (see below).

The isolated nature of the metallic sites was confirmed through STEM imaging, which revealed the absence of aggregates on the as-prepared catalysts. At high magnifications attainable through aberration corrected annular dark field STEM (AC-ADF-STEM), features of 0.2 nm assigned to palladium atoms could be visualised directly. For both Pd/NC and PdCu/NC, EDX maps showed that the respective metals were uniformly distributed across the sample (Fig. 3a and b). The electronic structure of surface palladium species obtained from XPS[37] for both catalysts evidenced a positive oxidation state (Fig. 3c), as reported previously, where Pd/NC had a higher Pd^{4+} content than PdCu/NC.[30] This characteristic feature of isolated atomic sites[38] extended to palladium SACs on Al_2O_3, AC, and ECN, with minor variations in the ratio of Pd^{4+} to Pd^{2+} (Fig. S6†). Analysis of the photoionisation spectra of copper in the $3p_{5/2}$ region (Fig. 3d) and the LMM Auger peak (Fig. 3e) revealed predominantly Cu^{2+} species, which could be formed from sample exposure to air.[39] Concurrently, analysis of the X-ray absorption near-edge structure (XANES) of the palladium and copper edges corroborated the positively-charged nature of palladium determined through XPS. The palladium K-edge revealed predominantly positively-charged palladium in both Pd/NC and PdCu/NC and matched the expected curve shape (Fig. 3f).[40] Remarkably, both spectra were virtually identical. The contribution of positively charged Pd (PdO reference) obtained from linear combination fitting (LCF) was similar for Pd/NC (91%) and PdCu/NC (86%), respectively, confirming the comparable electronic features of palladium in both catalysts. The contribution of cationic species coincides well with the ones derived from XPS (Pd/NC, 87% and PdCu/NC, 80%). The Fourier-transformed extended X-ray absorption fine structure (EXAFS) of both Pd/NC and PdCu/NC evidenced exclusively metal–nitrogen/oxygen paths (Pd–O/N, bond distance of 1.97 Å), with a coordination number of 2.5 (Fig. 3g, k-windows in Fig. S7†). The observations agree well with previously reported materials,[40] further highlighting the high dispersion of the palladium species. A similar analysis of the XANES at the copper edge (Fig. 3h) revealed predominantly positively-charged species (Cu^{2+}:58%, Cu^{+}: 28%). The corresponding EXAFS (Fig. 3i) also showed predominantly Cu–O/N paths (bond distance of 1.91 Å). Coordination numbers (2.6) and distances, match the expected values, with potentially minor contributions from Cu_2O species (see Table S4† for full fitting parameters).[31]

Performance of SACs in Sonogashira coupling

The coupling of aryl alkynes with iodo aryls can be operated under Sonogashira (Pd–Cu cocatalysed) or Heck–Cassar (copper-free) conditions.[41] Using the Heck–Cassar protocol the SACs displayed limited activity, with only Pd/AC, Pd/Al_2O_3, and Pd/ECN evidencing minor conversion to the coupled product. In our experiments, the addition of copper in the form of CuI improved the activity of all catalysts. Hence the following discussion focuses on experiments using copper cocatalysts (*i.e.*, Sonogashira conditions). Commonly employed iodobenzene and phenylacetylene were used as representative, inactivated substrates. The choice of base and solvent (see below) was determined based on reaction condition optimisation and is well in line with reported procedures.[42] A set of standard conditions was established for all catalytic tests (Fig. 4a). Organometallic catalysts with commercially available ligands ($PdCl_2(PPh_3)_2$, $Pd(PPh_3)_4$), as well as commonly employed palladium salts ($Pd(OAc)_2$, OAc acetate), or palladium nanoparticles on charcoal (Pd_{NP}/C) were selected as benchmark

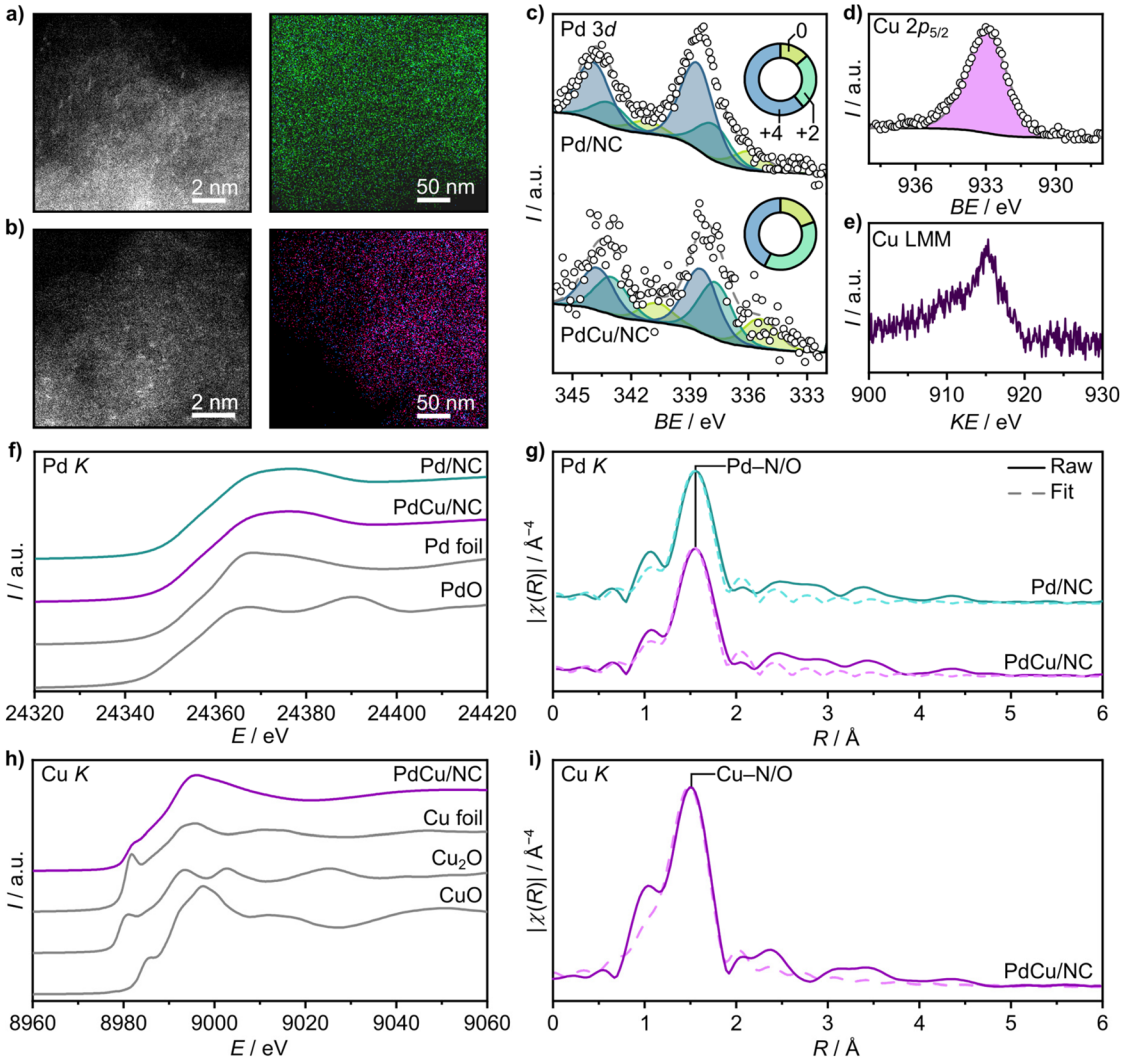

Fig. 3 AC-ADF-STEM images and EDX elemental maps of (a) Pd/NC and (b) PdCu/NC catalysts. Green, purple, and blue correspond to nitrogen, copper, and palladium in the elemental maps, respectively. (c) Pd 3*d* XPS (symbols) and corresponding fits (grey dashed line, coloured areas for individual components) of as-prepared Pd/NC and PdCu/NC. The doughnut plots inset show the relative distribution of the component fits. (d) Cu $2p_{5/2}$ with single peak fit and (e) LMM XPS of the as-prepared PdCu/NC catalyst. (f) Normalised palladium K-edge XANES and (g) Fourier-transformed EXAFS of Pd/NC and PdCu/NC with corresponding fits. (h) Normalised copper K-edge XANES and (i) Fourier-transformed EXAFS of PdCu/NC. The legend in (g) applies to (i).

systems. All molecular catalysts displayed significantly faster kinetics in the Sonogashira reaction compared to SACs, reaching quantitative conversion levels already after 2 h (Fig. 4b, only shown for $Pd(OAc)_2$), agreeing with previous reports.[43–45] Commercial Pd_{NP}/C had slightly lower activity below 1 h reaction time but still reached full conversion after 2 h. This material is known to evolve soluble palladium species through leaching, thus likely operating as a homogeneous catalyst. Similar reaction profiles were observed for SACs based on Al_2O_3 and AC (Fig. S8†), albeit reaching full conversion later (4 h and 6 h, respectively), which was later linked to the solubilisation of metal species (see below). Palladium leaching must occur within the first 15 minutes (for Pd_{NP}/C) to 2 h (for Pd/Al_2O_3 and Pd/AC) since no induction period is observed after the first sampling point.

In contrast, the rate of reaction over Pd/ECN and Pd/NC was much slower, reaching full iodobenzene only after 15 h (Pd/ECN, Fig. S8†), or only 80% conversion after 24 h (Pd/NC, Fig. 4b). The iodobenzene conversion over time decreases further when replacing the CuI cocatalyst with a fully heterogeneous, bimetallic PdCu/NC catalyst. For this material, the slow kinetics during the first 8 h likely reflects the absence of activated copper–alkyne complexes close to palladium centres. Similar activity differences between supported and dissolved copper entities have been previously observed in the Ullmann coupling reaction.[31] Evaluation of a copper single-atom catalyst based on NC evidenced no significant activity in the absence of palladium (4% yield).

For both Pd/NC and PdCu/NC, the selectivity to the desired product **3** was around 84 to 89% with net yields (*ca.* 70%)

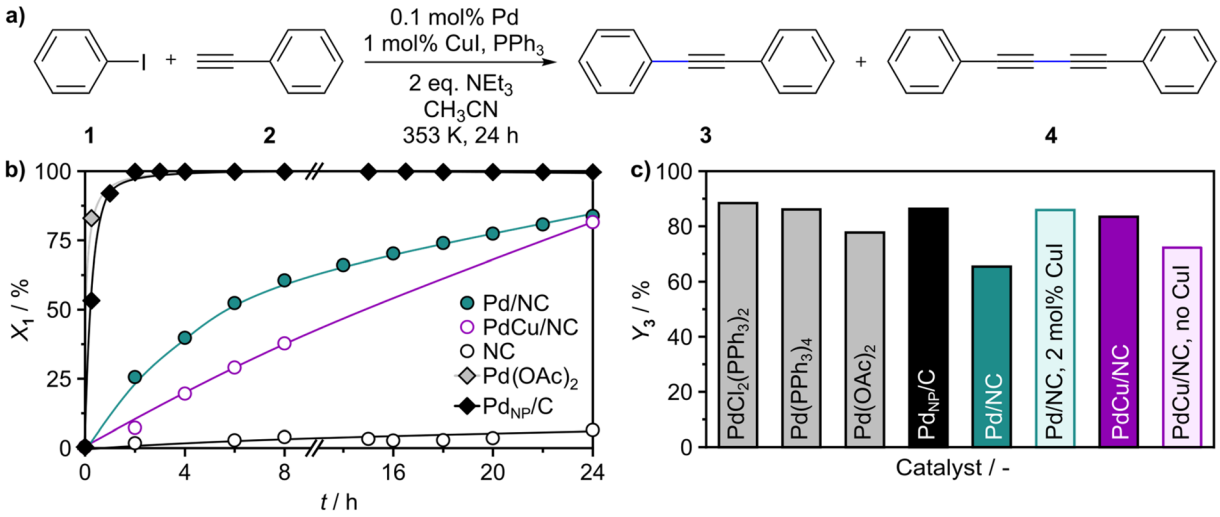

Fig. 4 (a) Standard reaction conditions for the Sonogashira cross-coupling of iodobenzene (1) and phenylacetylene (2), to the principal Sonogashira 3 and Glaser 4 coupling products. (b) Conversion of 1 (X_1) over time using Pd/NC and PdCu/NC (round symbols) and selected benchmarks (diamond symbols) under the reaction conditions indicated in (a). The metal-free carrier is shown for reference (open symbols). (c) Yield of 3 (Y_3) after 24 hours using selected benchmarks and Pd/NC and PdCu/NC catalysts under standard conditions unless otherwise specified.

lower than for organometallic benchmarks (*ca.* 80%, Fig. 4c). The yields of product **3** were matched using additional CuI for both Pd/NC (2 mol% added), and PdCu/NC (1 mol% added). The main side product 1,4-diphenyl-buta-1,3-diyne (**4**, Fig. 4a) was formed through copper-catalysed Glaser homocoupling of phenylacetylene (despite working under oxygen-free conditions),[46,47] whereas only traces of the dehalogenation product benzene were observed. Trace amounts of higher-order Glaser coupling products were also observed. Product isolation confirmed that the product distribution was adequately represented *via* GC analysis (Note S2†).

Taken together, the SACs displayed a distinct reactivity pattern compared to organometallic benchmark systems. A hybrid operation mode using copper in soluble form and Pd/NC was superior to using purely heterogeneous PdCu/NC.

Catalyst reuse and evolution

Heterogeneous catalysts must be separable without leaving palladium impurities in the product stream and ideally reusable to compete with the metal utilisation of more active organometallic benchmark systems. Palladium leaching from heterogeneous catalysts is a well-known issue in the literature, and leached species often mask the activity of the heterogeneous palladium sites.[15] Identifying the origin of palladium solubilisation among multiple reaction components is complex, but literature reports suggest that it occurs during the oxidative addition step of the aryl halide.[42,48] The LCA presented above underlines the importance of preventing metal loss during catalyst reuse.

To evaluate catalyst stability, fixed amounts of the initial Pd/NC catalysts were recovered and reused in three consecutive runs (Fig. 5a). Special attention was paid to avoid operating in a reactant-limited regime (*i.e.*, quantitative conversion). The yield to product **3** experienced a moderate decrease from *ca.* 70% to 55% under standard conditions. With an associated GWP of 5.6×10^{-2} $ton_{CO2\text{-}eq}$ $ton_{(3)}^{-1}$ the presented catalyst would have an environmental footprint between 4 to 60 times lower than the benchmark system. The fully bimetallic PdCu/NC displayed similar deactivation behaviour but required the addition of CuI to counteract extensive copper loss. Comparatively, SACs based on AC and ECN exhibited severe activity losses already after one catalytic run (Fig. S8†), which agrees with the palladium leaching evidenced after the first run. For context, the palladium loss from the commercial Pd_{NP}/C catalyst was almost quantitative after one run under the conditions employed.

The bulk metal content was monitored in the as-prepared (-R0) and reused monometallic Pd/NC catalyst samples, and displayed no significant changes in bulk metal content, strongly suggesting a lack of palladium leaching. There were no detectable traces of palladium in the corresponding liquid organic phases. Depending on the solubility of leached palladium species in the reaction medium, they may redeposit and form palladium nanoparticles under C–C cross-coupling reaction conditions. In line with the results above, palladium clusters were not observed in STEM images of the used Pd/NC and features assigned to palladium atoms could be readily visualised (Fig. 5b). As for other Pd-SACs, copper deposition was evidenced through EDX mappings, displaying a highly uniform elemental distribution without signs of aggregates. Analysis of the used catalysts by XPS displayed only minor changes in the speciation of Pd/NC (Fig. 5b), but stronger formation of reduced palladium species for the other recycled Pd SACs (Fig. S9†). XANES of Pd/NC after one (-R1) and three runs (-R3) revealed virtually no change in the oxidation state of palladium, however, a new feature located at 2–3 Å found in the

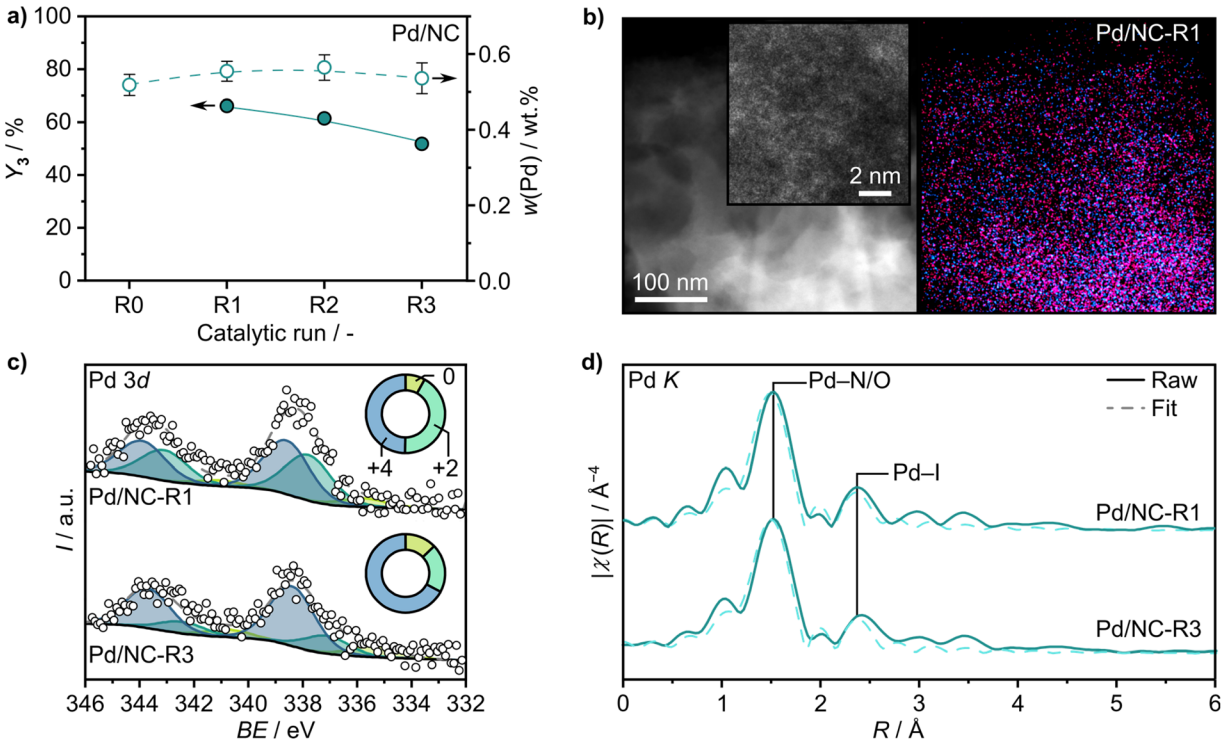

Fig. 5 (a) Yield of coupling product 3 (Y_3), and bulk palladium content of the catalyst (w(Pd)) during consecutive runs (as-prepared catalyst shown at R0) of the Sonogashira reaction over Pd/NC. The error bars show metal content variations falling within the detection limit of the instrument. (b) Pd 3*d* XPS spectra of Pd/NC after one (-R1) or three runs (R2) with the respective contributions of the fitted components (coloured areas) shown inset. (c) HAADF-STEM images and corresponding EDX elemental maps (Pd: blue, Cu: purple) of Pd/NC. A high-magnification AC-ADF-STEM image of Pd/NC displaying features associated with palladium atoms (size approximately 0.3 nm) is shown inset. (d) Magnitude of Fourier transformed EXAFS of used Pd/NC catalysts with corresponding fits in the *R*-space. The positions of Pd–O/N, and Pd–I shells are highlighted. Standard reaction conditions in all cases: 353 K, 0.1 mol% Pd, 1 mol% CuI, 2 eq. NEt_3, 24 h.

Fourier-transformed EXAFS suggests the formation of Pd–I (Fig. 5d). The Pd–N/O coordination remained largely unchanged (coordination number 2.4–2.5) and low coordination numbers of Pd–I (0.2) indicated low concentrations (Table S4†). The deposition of iodine on the catalyst surface caused by CuI was corroborated by EDX and XPS (Table S3†); the concentration of phosphorus from PPh_3 was negligible. The elemental uniformity, as well as the lack of larger palladium aggregates, for all SACs except for Pd/ECN, where a few larger particles were observed (Fig. S10†). Hence, the conditions employed did not favour palladium nanoparticle formation, and the removed metal was likely stabilised in ionic form (*e.g.*, through PPh_3) and washed out.

Besides metal leaching, another possible cause of deactivation is restructuring due to the interaction with components of the reaction medium. For example, solubilised copper species from CuI have previously been shown to adsorb onto exfoliated carbon nitride supports in the arylation of amines.[31] In particular, the Pd/NC and Pd/ECN catalysts experienced appreciable uptakes of copper (up to 1.5 wt% after three catalytic runs for Pd/NC, Table S5.† Analysis of the Cu $2p_{5/2}$ XPS spectra of the used catalysts showed that the adsorbed copper species have a Cu^{2+} character (932.5 eV, Fig. S9†), likely stemming from derivatives of deposited CuI.[39] Active site blockage due to fouling by copper does not appear to be the reason for the observed deactivation since the copper species appeared to be highly dispersed over the catalyst carriers and the surface copper content determined by XPS remained constant over consecutive runs (0.15 at%). Nonetheless, the effect of copper accumulation cannot be completely ruled out as the cause of the gradual activity loss, *e.g.*, through specific deposition of insoluble copper acetylide formed from CuI with phenylacetylene.[46] Further work is required to fully optimise reaction conditions in order to achieve quantitative yields. From the presented results, we propose (i) hybrid operation of Pd/NC with soluble CuI, (ii) optimisation of catalyst amount to the type of halide used, and (iii) solvent and base selection tailored to substrates of interest.

Conclusions and outlook

In conclusion, the integration of life cycle analysis with the experimental investigation of catalytic materials provided new perspectives on the selection and design of palladium single-atom heterogeneous catalysts as replacements for conventional homogeneous systems in Sonogashira coupling. The LCA

showed that solid catalysts could reduce the environmental footprint in terms of global warming potential, and endpoints in human health, ecosystems quality, and resources up to two orders of magnitude compared to business as usual. The environmental benefit of operating a heterogeneous catalyst tolerated some degree of catalyst deactivation but would be severely diminished by palladium leaching. From a range of catalytic materials, palladium single-atom catalysts based on nitrogen-doped carbon were shown to be active and highly stable to metal leaching when applied in a hybrid process in combination with a CuI cocatalyst. The characterisation results confirmed the isolated nature, as well as the expected electronic fingerprints of the metal sites. Benchmarking against representative organometallic catalysts under optimised conditions showed that the Pd/NC catalyst could match the Sonogashira product yield of homogeneous catalysts, albeit with slower kinetics. Upon catalyst reuse, the monometallic catalyst did not suffer from measurable palladium leaching in three consecutive catalytic runs. Despite moderate deactivation, as little as two recycles were sufficient to improve the GWP 4 to 60 times over the homogeneous catalyst. Attempts to develop a fully heterogeneous catalytic process using a bimetallic Pd–Cu single-atom catalyst failed due to extensive leaching of copper, which led to rapid deactivation in consecutive runs. Hence, the Pd/NC SAC presents a promising strategy for the implementation of solid catalysts in C–C cross-coupling transformations. In future work, the presented LCA framework may inform catalyst design and help streamline research efforts toward more sustainable catalytic materials.

Data availability statement

The datasets supporting this article are made available through Zenodo at **https://doi.org./10.5281/zenodo.6135989**.

Conflicts of interest

There are no conflicts to declare.

Acknowledgements

This publication was created as part of NCCR Catalysis (grant 180544), a National Centre of Competence in Research funded by the Swiss National Science Foundation. Christian Zaubitzer for training in STEM analysis and ScopeM at ETH Zurich for use of their facilities. Simon Büchele and Aviv Yarom for assistance with XPS measurements and data analysis, respectively.

Notes and references

1 K. Sonogashira, Y. Tohda and N. Hagihara, *Tetrahedron Lett.*, 1975, **16**, 4467–4470.
2 J. M. Murithi, C. Pascal, J. Bath, X. Boulenc, N. F. Gnädig, C. F. A. Pasaje, K. Rubiano, T. Yeo, S. Mok, S. Klieber, P. Desert, M. B. Jiménez-Díaz, J. Marfurt, M. Rouillier, M. H. Cherkaoui-Rbati, N. Gobeau, S. Wittlin, A. C. Uhlemann, R. N. Price, G. Wirjanata, R. Noviyanti, P. Tumwebaze, R. A. Cooper, P. J. Rosenthal, L. M. Sanz, F. J. Gamo, J. Joseph, S. Singh, S. Bashyam, J. M. Augereau, E. Giraud, T. Bozec, T. Vermat, G. Tuffal, J. M. Guillon, J. Menegotto, L. Sallé, G. Louit, M. J. Cabanis, M. F. Nicolas, M. Doubovetzky, R. Merino, N. Bessila, I. Angulo-Barturen, D. Baud, L. Bebrevska, F. Escudié, J. C. Niles, B. Blasco, S. Campbell, G. Courtemanche, L. Fraisse, A. Pellet, D. A. Fidock and D. Leroy, *Sci. Transl. Med.*, 2021, **13**, eabg6013.
3 J. W. B. Cooke, R. Bright, M. J. Coleman and K. P. Jenkins, *Org. Process Res. Dev.*, 2001, **5**, 383–386.
4 A. C. F. Cruz, E. M. Mateus and M. J. Peterson, *Org. Process Res. Dev.*, 2021, **25**, 668–678.
5 C. J. Barnett, T. M. Wilson and M. E. Kobierski, *Org. Process Res. Dev.*, 1999, **3**, 184–188.
6 K. D. Rollins and C. Lindley, *Clin. Ther.*, 2005, **27**, 1343–1382.
7 J. Magano and J. R. Dunetz, *Chem. Rev.*, 2011, **111**, 2177–2250.
8 D. Barbaras, J. Brozio, I. Johannsen and T. Allmendinger, *Org. Process Res. Dev.*, 2009, **13**, 1068–1079.
9 C. E. Garrett and K. Prasad, *Adv. Synth. Catal.*, 2004, **346**, 889–900.
10 S. Handa, Y. Wang, F. Gallou and B. H. Lipshutz, *Science*, 2015, **349**, 1087–1091.
11 B. Jin, F. Gallou, J. Reilly and B. H. Lipshutz, *Chem. Sci.*, 2019, **10**, 3481–3485.
12 S. Handa, J. D. Smith, Y. Zhang, B. S. Takale, F. Gallou and B. H. Lipshutz, *Org. Lett.*, 2018, **20**, 542–545.
13 M. Pagliaro, V. Pandarus, R. Ciriminna, F. Béland and P. Demma Carà, *ChemCatChem*, 2012, **4**, 432–445.
14 Z. Novák, A. Szabó, J. Répási and A. Kotschy, *J. Org. Chem.*, 2003, **68**, 3327–3329.
15 N. T. S. Phan, M. Van Der Sluys and C. W. Jones, *Adv. Synth. Catal.*, 2006, **348**, 609–679.
16 A. Biffis, P. Centomo, A. Del Zotto and M. Zecca, *Chem. Rev.*, 2018, **118**, 2249–2295.
17 L. Djakovitch and P. Rollet, *Adv. Synth. Catal.*, 2004, **346**, 1782–1792.
18 D. Ott, D. Kralisch, I. Denčić, V. Hessel, Y. Laribi, P. D. Perrichon, C. Berguerand, L. Kiwi-Minsker and P. Loeb, *ChemSusChem*, 2014, **7**, 3521–3533.
19 J. D. Hayler, D. K. Leahy and E. M. Simmons, *Organometallics*, 2019, **38**, 36–46.
20 P. T. Benavides, D. C. Cronauer, F. Adom, Z. Wang and J. B. Dunn, *Sustainable Mater. Technol.*, 2017, **11**, 53–59.
21 J. W. H. Burnett, Z. Sun, J. Li, X. Wang and X. Wang, *Green Chem.*, 2021, **23**, 7162–7169.
22 R. Rodríguez, J. J. Espada, M. I. Pariente, J. A. Melero, F. Martínez and R. Molina, *J. Cleaner Prod.*, 2016, **124**, 21–29.

23 C. S. Slater, M. J. Savelski and M. N. Ruiz-Felix, *J. Environ. Sci. Health, Part A: Toxic/Hazard. Subst. Environ. Eng.*, 2013, **48**, 1602–1608.
24 M. L. Parisi, A. Dessì, L. Zani, S. Maranghi, S. Mohammadpourasl, M. Calamante, A. Mordini, R. Basosi, G. Reginato and A. Sinicropi, *Front. Chem.*, 2020, **8**, 214.
25 P. Jessop, *Green Chem.*, 2020, **22**, 13–15.
26 S. K. Kaiser, Z. Chen, D. Faust Akl, S. Mitchell and J. Pérez-Ramírez, *Chem. Rev.*, 2020, **120**, 11703–11809.
27 Z. Chen, E. Vorobyeva, S. Mitchell, E. Fako, M. A. Ortuño, N. López, S. M. Collins, P. A. Midgley, S. Richard, G. Vilé and J. Pérez-Ramírez, *Nat. Nanotechnol.*, 2018, **13**, 702–707.
28 G. Ding, L. Hao, H. Xu, L. Wang, J. Chen, T. Li, X. Tu and Q. Zhang, *Commun. Chem.*, 2020, **3**, 43.
29 X. Zhang, Z. Sun, B. Wang, Y. Tang, L. Nguyen, Y. Li and F. F. Tao, *J. Am. Chem. Soc.*, 2018, **140**, 954–962.
30 S. Büchele, Z. Chen, S. Mitchell, R. Hauert, F. Krumeich and J. Pérez-Ramírez, *ChemCatChem*, 2019, **11**, 2812–2820.
31 E. Vorobyeva, V. C. Gerken, S. Mitchell, A. Sabadell-Rendón, R. Hauert, S. Xi, A. Borgna, D. Klose, S. M. Collins, P. A. Midgley, D. M. Kepaptsoglou, Q. M. Ramasse, A. Ruiz-Ferrando, E. Fako, M. A. Ortuño, N. López, E. M. Carreira and J. Pérez-Ramírez, *ACS Catal.*, 2020, **10**, 11069–11080.
32 ISO 14044:2006: Environmental management – Life Cycle Assessment: Requirements and guidelines, **https://www.iso.org/standard/38498.html**, (accessed February 2022).
33 G. Wernet, S. Conradt, H. P. Isenring, C. Jiménez-González and K. Hungerbühler, *Int. J. Life Cycle Assess.*, 2010, **15**, 294–303.
34 Z. Chen, S. Mitchell, E. Vorobyeva, R. K. Leary, R. Hauert, T. Furnival, Q. M. Ramasse, J. M. Thomas, P. A. Midgley, D. Dontsova, M. Antonietti, S. Pogodin, N. López and J. Pérez-Ramírez, *Adv. Funct. Mater.*, 2017, **27**, 1605785.
35 M. Rzelewska and M. Regel-Rosocka, *Phys. Sci. Rev.*, 2019, **3**, 1–27.
36 Ş. Sarioğlan, *Platinum Met. Rev.*, 2013, **57**, 289–296.
37 N. Hellgren, R. T. Haasch, S. Schmidt, L. Hultman and I. Petrov, *Carbon*, 2016, **108**, 242–252.
38 P. J. Schmitz, K. Otto and J. E. de Vries, *Appl. Catal., A*, 1992, **92**, 59–72.
39 M. C. Biesinger, *Surf. Interface Anal.*, 2017, **49**, 1325–1334.
40 E. Vorobyeva, E. Fako, Z. Chen, S. M. Collins, D. Johnstone, P. A. Midgley, R. Hauert, O. V. Safonova, G. Vilé, N. López, S. Mitchell and J. Pérez-Ramírez, *Angew. Chem., Int. Ed.*, 2019, **58**, 8724–8729.
41 L. Cassar, *J. Organomet. Chem.*, 1975, **93**, 253–257.
42 R. Chinchilla and C. Nájera, *Chem. Rev.*, 2007, **107**, 874–922.
43 J. L. Bolliger and C. M. Frech, *Adv. Synth. Catal.*, 2009, **351**, 891–902.
44 D. A. Alonso, C. Nájera and M. C. Pacheco, *Adv. Synth. Catal.*, 2003, **345**, 1146–1158.
45 D. Wang and S. Gao, *Org. Chem. Front.*, 2014, **1**, 556–566.
46 C. Glaser, *Ber. Dtsch. Chem. Ges.*, 1869, **2**, 422–424.
47 I. J. S. Fairlamb, P. S. Bäuerlein, L. R. Marrison and J. M. Dickinson, *Chem. Commun.*, 2003, **3**, 632–633.
48 M. B. Thathagar, P. J. Kooyman, R. Boerleider, E. Jansen, C. J. Elsevier and G. Rothenberg, *Adv. Synth. Catal.*, 2005, **347**, 1965–1968.